



**University of  
Zurich**<sup>UZH</sup>

**Zurich Open Repository and  
Archive**

University of Zurich  
University Library  
Strickhofstrasse 39  
CH-8057 Zurich  
[www.zora.uzh.ch](http://www.zora.uzh.ch)

---

Year: 2020

---

## **PhotoTag: Photoactivatable Fluorophores for Protein Labeling**

Fay, Rachael ; Linden, Anthony ; Holland, Jason P

**Abstract:** We report experimental studies on the development of photoactivatable fluorophores for rapid, light-induced synthesis of protein conjugates. Proof-of-concept studies demonstrated that electronic excitation of photoactivatable BODIPY-ArN3 (1) in the presence of different proteins leads to efficient labeling in less than 10 min. After synthesis and isolation of the fluorescently tagged protein, photochemical conversion yields using human serum albumin and onartuzumab were  $47 \pm 7\%$  and  $42 \pm 5\%$ , respectively.

DOI: <https://doi.org/10.1021/acs.orglett.0c00957>

Posted at the Zurich Open Repository and Archive, University of Zurich

ZORA URL: <https://doi.org/10.5167/uzh-187052>

Journal Article

Accepted Version

Originally published at:

Fay, Rachael; Linden, Anthony; Holland, Jason P (2020). PhotoTag: Photoactivatable Fluorophores for Protein Labeling. *Organic Letters*, 22(9):3499-3503.

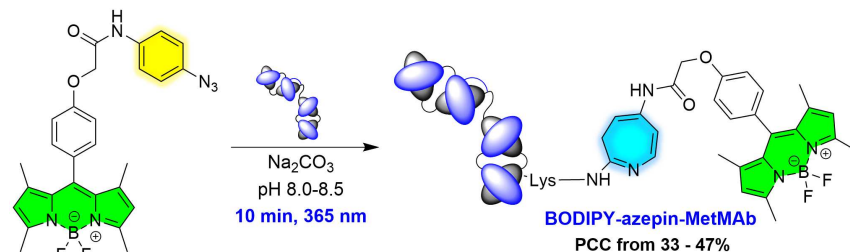
DOI: <https://doi.org/10.1021/acs.orglett.0c00957>

# PhotoTag – photoactivatable fluorophores for protein labelling

Rachael Fay<sup>a</sup>, Anthony Linden<sup>a</sup> and Jason P. Holland<sup>\*a</sup>

<sup>a</sup> University of Zurich, Department of Chemistry, Winterthurerstrasse 190, CH-8057, Zurich, Switzerland

Supporting Information Placeholder



**ABSTRACT:** We report experimental studies on the development of photoactivatable fluorophores for rapid, light-induced synthesis of protein-conjugates. Proof-of-concept studies demonstrated that electronic excitation of photoactivatable BODIPY-ArN<sub>3</sub> (**1**) in the presence of different proteins leads to efficient labelling in less than 10 minutes. After synthesis and isolation of the fluorescently-tagged protein, photochemical conversion yields (PCCs) using human serum albumin (HSA) and onartuzumab (MetMab<sup>TM</sup>) were  $47 \pm 7\%$ , and  $42 \pm 5\%$ , respectively.

Fluorescent protein-conjugates are vital tools in chemical and biomedical research. For instance, fluorescently-tagged antibodies (mAbs) are used in a wide range of applications, including substrate staining in gel-based assays, biomarker detection in tissue sections using immunohistochemistry and confocal fluorescence microscopy, cellular labelling in fluorescence assisted cell-sorting (FACS) and molecular imaging *in vivo* using fluorescence-mediated tomography (FMT).<sup>1</sup> Although inherently fluorescent proteins, such as green fluorescent protein (GFP), can be used for imaging, extrinsic labelling of non-emissive proteins with organic fluorophores provides access to a more diverse set of tools with control over their biological function and optical properties.<sup>2-4</sup>

Many organic small-molecule fluorophores have been employed for fluorescence-based detection methods. Commonly used dyes include the cyanine, fluorescein, rhodamine and BODIPY families.<sup>5,6</sup> The 4,4-difluoro-4-bora-3a,4a-diaza-*s*-indacene (BODIPY) scaffold offers several advantages for use in biological systems, including vivid chromophores, good fluorescence quantum yields, and high stability at physiological pH.<sup>7</sup> Auxochromic modifications can also be introduced to the BODIPY scaffold, thereby allowing the characteristic absorption and emission bands to be modulated to the more biologically suitable near infrared (NIR) region. For instance, the addition of thienyl groups on the pyrrole ring induces a bathochromic shift.<sup>8,9</sup>

Established methods for labelling biologically active molecules with derivatives of BODIPY (or other fluorophores) are usually based on thermochemically initiated reactions,

including modification of lysine residues with N-hydroxy-succinimide (NHS) and isothiocyanate (NCS)-activated BODIPY agents, cysteine-specific functionalization with maleimide-BODIPY, and copper-mediated ‘click’ chemistry with alkyne- or azide-functionalized BODIPY.<sup>10-16</sup> Reactions at cysteine residues often require the addition of a reducing agent to break disulfide bridges and reveal the reactive sulfhydryl groups. Although the ‘click’ approach is reliable and efficient, it requires multi-step chemistry involving pre-modification of the protein with either an alkyne or azide group, followed by bioorthogonal protein-functionalization with the fluorophore.<sup>17,18</sup> Both Michael addition to sulfhydryl groups and copper-mediated ‘click’ reactions require the use of potentially harsh, redox-active chemicals for the bioconjugation step (TCEP, DTT, THPTA,  $\text{CuSO}_4$ ), which has the potential to compromise the biological integrity and function of the protein by disrupting the tertiary structure.<sup>10,12</sup> To expand the scope of fluorescently labelled biomolecules, alternative strategies for tagging proteins are required. Ideally, new methods should be simple, efficient and reproducible, allowing for the rapid, one-step labelling of *unmodified* proteins with minimal intervention. Here, we report a new method to incorporate the BODIPY scaffold into biomolecules as another method to complement the existing toolbox of inherently and tagged fluorescent proteins.

Photochemistry offers a range of reagents and mechanisms with potential for use in light-induced protein-functionalization. For example, in 2015, Murale *et al.* reported the synthesis of an asymmetric photoactivatable BODIPY bearing a modified benzophenone motif attached to the 2- or 3-position of one of the

pyridyl groups.<sup>19</sup> Excitation of the aryl ketone likely produces a triplet biradical species, which was reported to allow photo-induced labelling of three different proteins, including HSA, bovine serum albumin (BSA) and lysozyme under UV irradiation. Although promising, the approach has several drawbacks. Specifically, photo-induced reactions gave very low efficiencies (typically 0.1 – 0.6%; with a maximum of 3.5% with tyrosine) and protein labelling yields were not reported, and photoexcitation required the use of UV light at wavelengths that are likely to damage the protein. To circumvent these issues, we report the synthesis of BODIPY-ArN<sub>3</sub>, in which the aryl azide (ArN<sub>3</sub>) group is distal to the BODIPY chromophore and is photoactivated at wavelengths (365 nm) that are not absorbed by most proteins, thereby avoiding detrimental photodegradation.

**Scheme 1.** Synthesis of BODIPY-ArN<sub>3</sub> (**1**). (i) acetic anhydride, cat. TFA, 2,4-dimethylpyrrole, DCM; (ii) DDQ, DCM/THF; (iii) NEt<sub>3</sub>, BF<sub>3</sub>OEt<sub>2</sub>, DCM; (iv) K<sub>2</sub>CO<sub>3</sub>, MeOH.

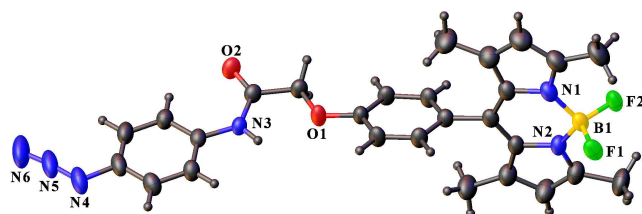
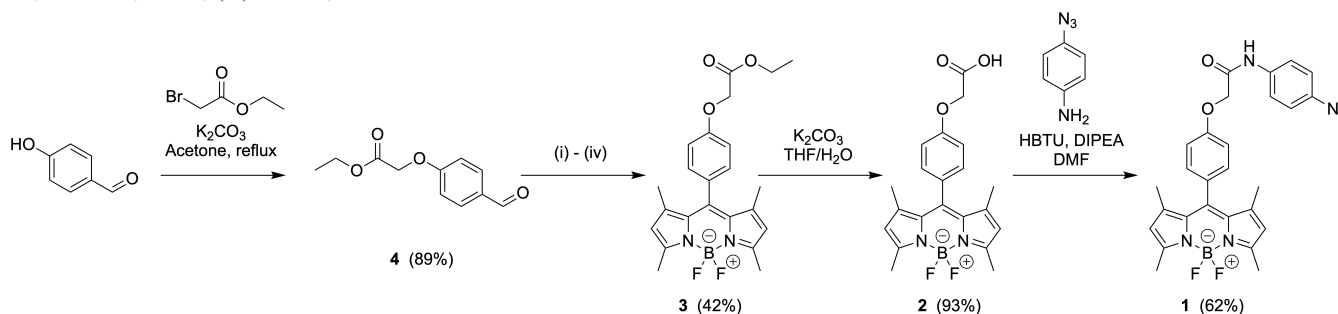


**Figure 1.** Single-crystal X-ray structure of BODIPY-ArN<sub>3</sub> (**1**) (see also Supporting Figure 24 for depiction of the thermal ellipsoids)

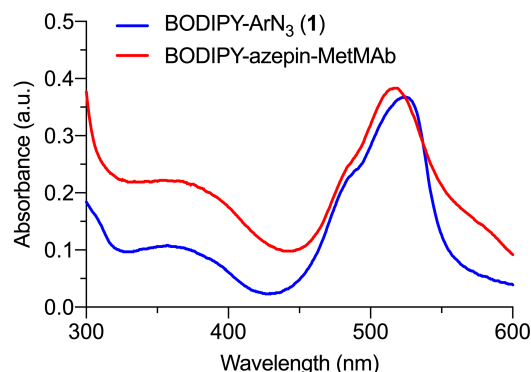


**Figure 2.** Electronic absorption (UV/vis) profile of (blue) BODIPY-ArN<sub>3</sub> (**1**) and (red) BODIPY-azepin-MetMAb.

The maximum excitation and emission wavelengths of compound **1** were determined to be 497.5 nm and 508.5 nm, respectively (Supporting Figure 12). The small Stokes shift (~11 nm)

BODIPY-ArN<sub>3</sub> (**1**) was synthesized in 4-steps starting from 4-hydroxybenzaldehyde and isolated with an overall yield of 22% (Scheme 1; Supporting Figures 1–14).<sup>20</sup> The ArN<sub>3</sub> group was installed in the final step by amide coupling with 4-azidoaniline hydrochloride in a yield of 62%. The single-crystal X-ray structure of compound **1** was also obtained (Figure 1 and Supporting Table 4). Full experimental details and characterization data including <sup>1</sup>H, <sup>19</sup>F and <sup>13</sup>C NMR, high-resolution mass spectrometry, electronic absorption (UV/vis) spectroscopy, fluorescence spectroscopy and X-ray crystallography data are presented in the supporting information.

is characteristic of BODIPY compounds, which undergo little change in geometry upon photoexcitation.<sup>21,22</sup> The quantum yield of compound **1** ( $\Phi$ ) was determined in 0.1 M NaOH relative to fluorescein and found to be 0.03 (Supporting Figure 13) which is within the wide range of previously reported quantum yields for BODIPY compounds.<sup>23–26</sup> The electronic absorption profile of compound **1** showed an intense band at the wavelength used for photo-activation, 365 nm ( $\epsilon = 10,500 \text{ M}^{-1} \text{ cm}^{-1}$ ; Figure 2; Supporting Figure 14 and Supporting Tables 1 and 2).

Light-induced activation of the *para*-substituted ArN<sub>3</sub> group initially leads to the formation a highly reactive open-shell singlet nitrene species after loss of N<sub>2</sub>(g).<sup>27</sup> The reactivity of aryl nitrenes is well-established.<sup>28</sup> It has a reported half-life on the order of a nanosecond and can react via several pathways, including H-atom abstraction, (C-H or X-H) bond insertion or intramolecular rearrangements to form a 7-membered ketenimine ring. This ketenimine species reacts readily with nucleophiles (including the  $\epsilon$ -NH<sub>2</sub> group of lysine) in a bimolecular reaction to form an azepine linkage between the protein and the ligand.<sup>29–32</sup> Although productive bimolecular reactions with primary amine groups of proteins appears to be favoured kinetically, the ketenimine intermediate can also reactions slowly with other nucleophiles, including nonproductive quenching with water.<sup>27,33</sup> Density functional theory (DFT) calculations were performed to investigate the mechanism and photochemical reaction coordinate of compound **1** (Supporting Table 3 and Supporting Figures 15–17). The DFT calculations revealed that rearrangement of the open-shell singlet nitrene (<sup>1</sup>A<sub>2</sub> state) to give the ketenimine is feasible and subsequent nucleophilic attack by primary amines is thermodynamically favored compared with attack by carboxylate groups.

Before testing protein-conjugation reactions, the photochemical reactivity of BODIPY-ArN<sub>3</sub> (**1**) was studied by using high-

performance liquid chromatography (HPLC). A solution of compound **1** (0.25 mM, in MeOH) was irradiated by using a high-powered light-emitting diode (LED, 365 nm; 263 mW) at room temperature. Aliquots of the photolysis reaction were analyzed by HPLC at time points from 0 to 5 min. (Figure 3A). As a control, the intermediate compound, BODIPY-OEt (**3**), which lacks the ArN<sub>3</sub> group, was also irradiated under equivalent conditions to determine if the BODIPY core was susceptible to photodegradation at 365 nm (Figure 3B). HPLC analysis indicated that after 4 minutes, compound **1** reacted completely to give one major species, which was more polar than the starting material. Intermediate **3** produced only minor impurities after 5 minutes of irradiation, which indicated that the BODIPY scaffold is stable to the irradiation conditions and that the light-induced reactivity of compound **1** is mediated by the ArN<sub>3</sub> group. Mass spectrometry data from the photolysed product

were consistent with the loss of N<sub>2</sub> and the formation of an azepine or related isomer (Supporting Figures 18 and 19).

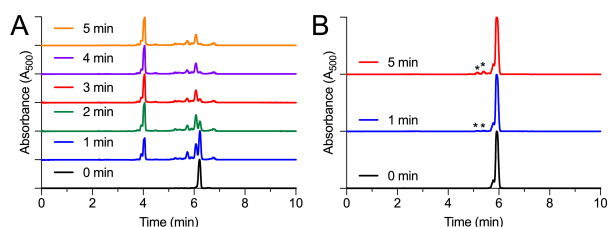
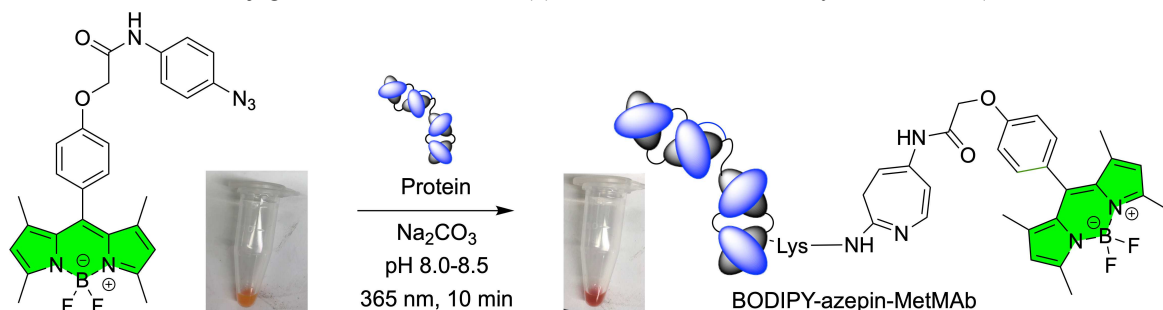


**Figure 3.** HPLC chromatograms showing photodegradation over time of (A) BODIPY-ArN<sub>3</sub> (**1**), and (B) BODIPY-OEt (**3**).

**Scheme 2.** Photochemical conjugation of BODIPY-ArN<sub>3</sub> (**1**) to the monovalent antibody onartuzumab (formulated as MetMab<sup>TM</sup>).



Next, we performed a series of experiments to determine if light-induced activation of BODIPY-ArN<sub>3</sub> (**1**) in the presence of protein could lead to the formation of fluorescent protein-conjugates. Two different proteins were studied: HSA and the humanized, monovalent engineered antibody onartuzumab (formulated as the pharmaceutical MetMab<sup>TM</sup>), which targets the human hepatocyte growth-factor receptor c-MET (Scheme 2).

Aliquots of BODIPY-ArN<sub>3</sub> (**1**, DMSO) were added to stock solutions of HSA (reconstituted in sterile saline; 69.08 kDa, 60 Lys,  $\epsilon_{280} = 36,500 \text{ M}^{-1} \text{ cm}^{-1}$ ) or MetMab<sup>TM</sup> (containing the native formulation buffer; 99.16 kDa, 66 Lys,  $\epsilon_{280} = 161,465 \text{ M}^{-1} \text{ cm}^{-1}$ ).<sup>34</sup> The pH of the protein solution was adjusted to 8.0-8.5 by using aliquots of Na<sub>2</sub>CO<sub>3</sub>. Solutions were mixed thoroughly before irradiation at 365 nm for 10 min at room temperature. Full experimental details are presented in the Supporting Information. After irradiation, proteins were purified from the small-molecule components by size-exclusion chromatography (SEC) using PD-10 columns eluted with PBS buffer (pH 7.4) (Supporting Figure 20). Purified proteins were collected in the high molecular weight fraction and analyzed by electronic absorption spectroscopy (Figure 2 (red)), gel electrophoresis (Figure 4 and Supporting Figures 21 and 22) and by using SEC coupled to HPLC (Supporting Figure 23). HPLC analysis and visual analysis confirmed that the protein-fraction (detected at  $\lambda = 280 \text{ nm}$ ) co-eluted with a peak observed in the 515 nm channel, which was assigned to the absorption of the BODIPY dye. However, to determine whether the dye was covalently bound to the protein and to exclude the possibility that the photo-BODIPY-ArN<sub>3</sub> was forming aggregates (or polymers) during irradiation that co-elute with the protein fraction, a control reaction where compound **1** was irradiated in the absence of protein was performed.

After irradiation, the reaction products were purified by PD-10 SEC and the fractions analyzed by fluorescence emission intensity. Analysis of the high molecular weight fraction from control reactions showed <8% of the total fluorescence intensity found in the protein-conjugation reactions with MetMab<sup>TM</sup> (Supporting Figure 19). These data confirmed that light-induced activation of BODIPY-ArN<sub>3</sub> in the presence of protein leads to specific protein functionalization.

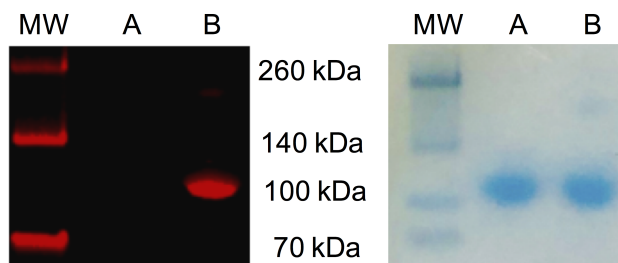


**Figure 4.** SDS Page analysis of (A) Unmodified MetMab, (B) BODIPY-azepin-MetMab analyzed by (left) fluorescence imaging showing pseudo-colored bands and (right) Coomassie staining.

Further confirmation of protein-conjugation was obtained by running samples of unfunctionalised MetMab<sup>TM</sup>, and photo-conjugated BODIPY-azepin-MetMab on SDS-PAGE in non-reducing conditions (Figure 4). Gels were first visualized by fluorescence imaging, followed by incubation with Coomassie to stain protein bands. Coomassie-stained gels showed one band for MetMab<sup>TM</sup> at approximately 100 kDa, which corresponds with the intact one-arm antibody (Figure 4, right lanes A and B). Fluorescent imaging showed a band that migrated to the

same position but corresponded with BODIPY-azepin-MetMab (Figure 4, left lane B). Gel-electrophoresis of BODIPY-azepin-HSA and BODIPY-azepin-MetMab run under reducing conditions are shown in Supporting Figures 20 and 21, respectively. The reducing SDS-PAGE of BODIPY-azepin-MetMab showed that both the light-chain and the heavy-chain are fluorescently labelled. Notably, under the conditions used for the gel-electrophoresis, non-covalently bound dye molecules are highly unlikely to remain bound to the protein.

After confirming the successful protein-conjugation, we next evaluated the photochemical conjugation efficiency (PCC; or yield) and the degree of labelling (D.O.L.) by using different stoichiometric equivalents of compound **1** (Table 1). To avoid

precipitation of the protein and to ensure that the DMSO content remained <10%, reactions using 10 equivalents of compound **1** were performed at lower protein concentrations. The D.O.L. was calculated from calibrated UV/vis spectra of the purified protein-conjugates by using Equation 1. From the experimental D.O.L., the yield could be calculated by division with the theoretical maximum yield.

$$D.O.L. = \frac{A_{max} \cdot \epsilon_{protein}}{(A_{280} - A_{max} C_{280}) \cdot \epsilon_{max}}, \text{ where } C_{280} = \frac{A_{280}(dye)}{A_{max}(dye)}$$

(Equation 1)

**Table 1.** Degree of labelling and photochemical conversion yields for the light-induced protein-conjugation reaction BODIPY-ArN<sub>3</sub> (**1**) with MetMab<sup>TM</sup> and HSA *versus* varying equivalents of compound **1**.

Protein	[protein] (μM)	Equivalents of <b>1</b>	D.O.L. average ± s.d (n = 3)	PCC yield ± s.d (%) (n = 3)
MetMab	168	2.5	0.82 ± 0.07	33 ± 3
	168	5	2.21 ± 0.24	42 ± 5
	101	10	4.06 ± 0.34	41 ± 3
HSA	208	2.5	1.17 ± 0.18	47 ± 7
	195	4.8	1.62 ± 0.28	34 ± 6
	96	10	1.84 ± 0.44	28 ± 4

Photochemical conversion efficiencies did not reach quantitative yields since other competing reactions exist. It has been reported that the ketenimine species can react slowly with water and O<sub>2</sub>.<sup>32,33</sup> It is possible that reactive nucleophiles (i.e. histidine) present in the formulation buffer of MetMab<sup>TM</sup> compete with lysine groups on the protein. In addition to intramolecular rearrangement to the ketenimine, the aryl nitrene species produced after photo-induced loss of N<sub>2</sub> can undergo intersystem crossing to give a triplet species or protonation to form a nitrenium ion which is unreactive towards amino acids.<sup>28</sup>

Photochemical conjugation to MetMab and HSA proceeded efficiently with slightly varying yields that were dependent on the initial equivalents of BODIPY-ArN<sub>3</sub> added. The PCC was calculated as the average (n = 3) ± the standard deviation (s.d.). HSA was labelled the most efficiently with 2.5 eq. of compound **1** (PCC = 47 ± 7%). MetMab<sup>TM</sup> could be labelled slightly more efficiently with a larger initial excess of compound **1** (5-10 equivalents). Our previous studies involving immunoreactivity measurements indicated that irradiation of MetMab<sup>TM</sup> at 365 nm does not compromise protein function.<sup>32</sup>

Light-induced protein-conjugation offers several advantages over existing coupling methods. First, reactions are extremely fast and run to completion in just a few minutes. Increased irradiation flux can also reduce reaction times.<sup>31</sup> Functionalisation requires only one-step from unmodified proteins and tolerates standard formulation buffers. The reaction is reproducible and proceeds in good PCC yields. Photoactivatable ArN<sub>3</sub> dyes are easy to synthesize, can be crystallized, are bench stable, and are not susceptible to hydrolysis. Finally, the conjugation process is simple and user-friendly, and unlike other modification chemistries, requires no additional protein handling steps, such as pre-purification or pre-functionalization. We continue to expand on these proof-of-concept studies by developing photoactivatable dyes (PhotoTags) using a range of fluorophore classes and different photoactive groups.

## ASSOCIATED CONTENT

### Supporting Information

A PDF of electronic supporting information file is available and contains details on the synthesis and characterization of all compounds. In addition, further experimental data on the reactivity of BODIPY-ArN<sub>3</sub> are presented in. DFT data are presented and further details of the single-crystal X-ray structure of compound **1** are given. CCDC accession number: 1950789

The Supporting Information is available free of charge on the ACS Publications website.

## AUTHOR INFORMATION

### Corresponding Author

\* Prof. Dr Jason P. Holland, E-mail: [jason.holland@chem.uzh.ch](mailto:jason.holland@chem.uzh.ch); Tel: +41446353990; Home page: [www.hollandlab.org](http://www.hollandlab.org)

### Author Contributions

Rachael Fay conducted and designed all experiments, analyzed the data and wrote the first draft. Prof. Dr Anthony Linden collected and analyzed the crystallography data. Prof. Dr Jason P. Holland supervised the project, designed experiments, analyzed data and wrote the manuscript. All authors corrected and approved the final version of this work.

## ACKNOWLEDGMENT

JPH thanks the Swiss National Science Foundation (SNSF Professorship PP00P2\_163683 and PP00P2\_190093), the European Research Council (676904, ERC-StG-2015, NanoSCAN), the Swiss Cancer League (KLS-4257-08-2017), and the University of Zurich for financial support.

## REFERENCES

- (1) Hoffman, R. M. *Nat. Rev. Cancer* **2005**, 5 (10), 796.



- (2) Crivat, G.; Taraska, J. W. *Trends in Biotechnology*. January 2012, pp 8–16.
- (3) Fujiki, Y.; Tao, K.; Bianchi, D. W.; Giel-Moloney, M.; Leiter, A. B.; Johnson, K. L. *Cytometry. A* **2008**, *73* (2), 11.
- (4) Bozhanova, N. G.; Baranov, M. S.; Klementieva, N. V.; Sarkisyan, K. S.; Gavrikov, A. S.; Yampolsky, I. V.; Zagaynova, E. V.; Lukyanov, S. A.; Lukyanov, K. A.; Mishin, A. S. *Chem. Sci.* **2017**, *8* (10), 7138.
- (5) Kowada, T.; Maeda, H.; Kikuchi, K. *Chemical Society Reviews*. Royal Society of Chemistry July 2015, pp 4953–4972.
- (6) Suzuki, T.; Matsuzaki, T.; Hagiwara, H.; Aoki, T.; Takata, K. *Acta Histochemica et Cytochemica*. 2007, pp 131–139.
- (7) Ni, Y.; Wu, J. *Organic and Biomolecular Chemistry*. Royal Society of Chemistry June 2014, pp 3774–3791.
- (8) Leushina, E. A.; Usol'tsev, I. A.; Bezzubov, S. I.; Moiseeva, A. A.; Terenina, M. V.; Anisimov, A. V.; Taydakov, I. V.; Khoroshutin, A. V. *Dalt. Trans.* **2017**, *46* (48), 17093.
- (9) Li, G.; Otsuka, Y.; Matsumiya, T.; Suzuki, T.; Li, J.; Takahashi, M.; Yamada, K. *Materials (Basel)*. **2018**, *11* (8).
- (10) Matsumoto, T.; Urano, Y.; Shoda, T.; Kojima, H.; Nagano, T. *Org. Lett.* **2007**, *9* (17), 3375.
- (11) Chauhan, D. P.; Saha, T.; Lahiri, M.; Talukdar, P. *Tetrahedron Lett.* **2014**, *55* (1), 244.
- (12) Cheng, M. H. Y.; Savoie, H.; Bryden, F.; Boyle, R. W. *Photochem. Photobiol. Sci.* **2017**, *16* (8), 1260.
- (13) Tyagarajan, K.; Pretzer, E.; Wiktorowicz, J. E. *Electrophoresis* **2003**, *24* (14), 2348.
- (14) Albrecht, M.; Lippach, A.; Exner, M. P.; Jerbi, J.; Springborg, M.; Budisa, N.; Wenz, G. *Org. Biomol. Chem.* **2015**, *13* (24), 6728.
- (15) Rezende, L. C. D. D. L.; Emery, S.; Emery, F. *Orbital Elec. J. Chem* **2013**, *5* (1), 62.
- (16) Ono, M.; Watanabe, H.; Ikehata, Y.; Ding, N.; Yoshimura, M.; Sano, K.; Saji, H. *Sci. Rep.* **2017**, *7* (1).
- (17) Pickens, C. J.; Johnson, S. N.; Pressnall, M. M.; Leon, M. A.; Berkland, C. J. *Bioconjugate Chemistry*. American Chemical Society March 2018, pp 686–701.
- (18) Lang, K.; Chin, J. W. *Chemical Reviews*. American Chemical Society May 2014, pp 4764–4806.
- (19) Murale, D. P.; Hong, S. C.; Yun, J. H.; Yoon, C. N.; Lee, J. S. *Chem. Commun.* **2015**, *51* (30), 6643.
- (20) Sampedro, A.; Villalonga-Planells, R.; Vega, M.; Ramis, G.; Fernández De Mattos, S.; Villalonga, P.; Costa, A.; Rotger, C. *Bioconjug. Chem.* **2014**, *25* (8), 1537.
- (21) Zhu, X. Y.; Yao, H. W.; Fu, Y. J.; Guo, X. F.; Wang, H. *Anal. Chim. Acta* **2019**, *1048*, 194.
- (22) Thakare, S. S.; Chakraborty, G.; More, A. B.; Chattopadhyay, S.; Mula, S.; Ray, A. K.; Sekar, N. *J. Lumin.* **2018**, *194*, 622.
- (23) Kuhn, H. J.; Braslavsky, S. E.; Schmidt, R. *Pure Appl. Chem.* **2004**, *76* (12), 2105.
- (24) Brouwer, A. M. *Pure and Applied Chemistry*. 2011, pp 2213–2228.
- (25) Boens, N.; Leen, V.; Dehaen, W. *Chem. Soc. Rev.* **2012**, *41* (3), 1130.
- (26) Loudet, A.; Burgess, K. *Chemical Reviews*. November 2007, pp 4891–4932.
- (27) Preston, G. W.; Wilson, A. J. *Chem. Soc. Rev.* **2013**, *42* (8), 3289.
- (28) Gritsan, N. P.; Platz, M. S. *Chem. Rev.* **2006**, *106* (9), 3844.
- (29) Voskresenska, V.; Wilson, R. M.; Panov, M.; Tarnovsky, A. N.; Krause, J. A.; Vyas, S.; Winter, A. H.; Hadad, C. M. *J. Am. Chem. Soc.* **2009**, *131* (32), 11535.
- (30) Eichenberger, L. S.; Patra, M.; Holland, J. P. *Chem. Commun.* **2019**, *55*, 2257.
- (31) Patra, M.; Eichenberger, L. S.; Fischer, G.; Holland, J. P. *Angew. Chemie Int. Ed.* **2019**, *58*, 1928.
- (32) Fay, R.; Gut, M.; Holland, J. P. *Bioconjug. Chem.* **2019**, *30*, 1814.
- (33) Platz, M. S. *Acc. Chem. Res.* **1995**, *28* (12), 487.
- (34) Bateman, A. *Nucleic Acids Res.* **2019**, *47* (D1), D506.